(Received 11 June 2024, Accepted 12 July 2024, Scheduled 20 July 2024)

A Dual-Notched Ultra-Wideband Monopole Antenna Based on Frequency Selective Surface Technology

Yingjie Du[1] and Mingxin Liu[1, 2, 3, *]

[1] School of Aviation Maintenance Engineering, Chengdu Aeronautic Polytechnic, Chengdu 610100, Sichuan, China
[2] School of Aeronautics and Astronautics
University of Electronic Science and Technology of China, Chengdu 611731, Sichuan, China
[3] Postdoctoral Innovation Practice Base, Chengdu Textile College, Chengdu 611731, Sichuan, China

ABSTRACT: To solve the problem of antenna miniaturization and mutual interference between the communication band of the UWB system and other wireless communication system bands, this paper proposes a UWB monopole antenna which has frequency notch characteristics. By applying two pairs of Split Ring Resonator (SRR) structures on a CPW transmission line, a coupling resonance is generated in a specific frequency band, and the antenna has a dual frequency notch and a wide band notch function. The measured results show that the antenna has good band-notch characteristics in the frequency ranges of 3.3 GHz to 4 GHz and 5.1 GHz to 6.2 GHz, suppressing ultra-wideband interference between WiMAX (3.3 GHz $\sim$ 3.8 GHz) and WLAN (5.15 GHz $\sim$ 5.35 GHz and 5.725 GHz $\sim$ 5.825 GHz) in a wireless communication system. The volume of the antenna is 40 mm $\times$ 36 mm $\times$ 1 mm, and the measured results are compared with the simulated model results. Besides, the measured and simulated results have a good consistency.

1. INTRODUCTION

With the rapid development of wireless communication systems, ultra-wideband (UWB) antennas have become a focal point in the field of wireless communication and have gained increasing attention from researchers and designers. In recent years, various low-cost and compact structures have been proposed and applied to UWB antenna designs [1–6]. However, UWB communication systems often coexist with narrowband communication frequency bands, such as Worldwide Interoperability for Microwave Access (WiMAX) (3.3 GHz $\sim$ 3.8 GHz) and Wireless Local Area Networks (WLAN) (5.15 GHz $\sim$ 5.35 GHz and 5.725 GHz $\sim$ 5.825 GHz). To prevent mutual interference between UWB communication systems and other narrowband communication frequency bands, it is desirable to design UWB antennas with notch characteristics. Researchers have conducted in-depth studies on UWB antenna designs with notch characteristics. In [7], a dual-notch effect was achieved on a circular patch by etching open and π-shaped slots on a microstrip feed line. In [8], multiple notch effects were obtained by using partially slotted ground layers and capacitively loaded loops. Ref. [9] presents a dual-notch UWB antenna designed with an improved electromagnetic bandgap structure. In [10], notch characteristics were achieved by slotting on a U-shaped radiation patch. Most of these methods for achieving multiple notches involve etching slots or loading notch structures on radiation patches or transmission lines.

This paper introduces the principle of Split Ring Resonator (SRR) and presents the design of a UWB antenna with notch characteristics by incorporating two pairs of SSRs on a monopole antenna. The designed antenna provides notch frequencies that cover the WiMAX (3.3 GHz $\sim$ 3.8 GHz) and WLAN (5.15 GHz $\sim$ 5.825 GHz) frequency bands. The antenna dimensions are optimized through simulations to be 40 mm $\times$ 36 mm $\times$ 1 mm. After fabrication and testing, the antenna exhibits a reflection coefficient of $S_{11} < -10$ dB in the frequency bands of 2.1 GHz to 3.3 GHz, 4.1 GHz to 5.1 GHz, and 6.3 GHz to 10.8 GHz, except for the notch frequencies, where $S_{11} > -10$ dB, indicating effective band-notch characteristics.

2. DESIGN AND PRINCIPLE OF THE SSRS

The prototype antenna design presented in this paper is a rectangular monopole antenna fed by a coplanar waveguide (CPW), which achieves omnidirectional radiation characteris-

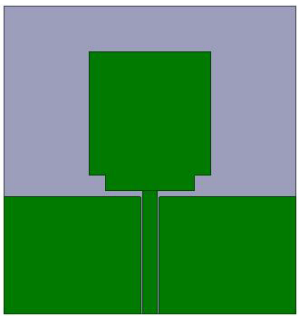

FIGURE 1. Structure diagram of the UWB monopole antenna.

* Corresponding author: Mingxin Liu (lmx0951@163.com).

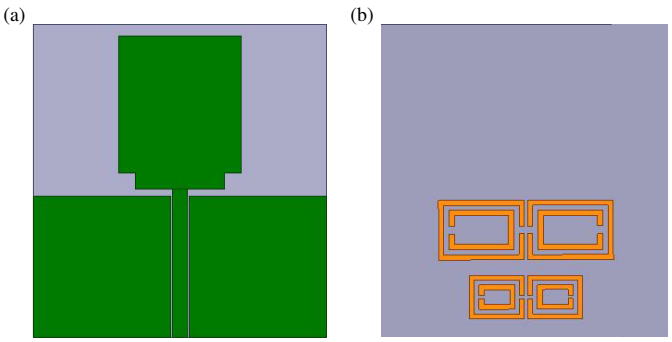

FIGURE 2. Structure diagram of the UWB bandstop antenna. (a) Front, (b) back.

tics in space. Figure 1 illustrates the structural diagram of the prototype UWB antenna (Antenna 1).

Figure 2 depicts the structural diagram of the wideband antenna designed in this paper, which exhibits dual-notch characteristics. The antenna radiator is a square monopole antenna with a lower notch, fed by CPW. The antenna is printed on an FR4 substrate with a thickness of 1 mm, a dielectric constant of 4.4, and a dielectric loss tangent of 0.02. Two pairs of SSRs are loaded on both sides of the CPW backplane to achieve dual-band notch characteristics.

Figure 2(b) illustrates the uniform symmetric distribution of two square SRRs printed on the backplane of the CPW, which are magnetically coupled with the CPW feed line. By adjusting the structural dimensions of the SSRs, broadband multi-band rejection characteristics can be realized. When the CPW signal line propagates electromagnetic waves, the magnetic field couples into the SSRs through their central axis. The varying magnetic field induces currents on the open resonant metal rings. Due to the relative positions of the inner and outer rings, opposite charges accumulate on the same side of the inner and outer rings, leading to displacement currents between the inner and outer rings. Consequently, the gap between the inner and outer rings forms a distributed capacitance. Additionally, the current loop itself acts as an equivalent distributed inductance, causing the SSRs to resonate at specific frequencies. At this point, the SSRs act as magnetic dipoles [11].

In general, the propagation of electromagnetic signals on the CPW induces an electromotive force on the SRRs, which, in turn, causes the currents between the two rings of the SRRs to flow in opposite directions. This excitation leads to resonance in the stimulated SRRs and prevents the propagation of electromagnetic waves on the CPW transmission line at their resonant frequencies, resulting in a notch effect for the wideband antenna at specific frequencies. The resonant frequency can be determined by calculating the distributed capacitance between the rings and the inductance of the SRR, and it is a function of the geometric parameters of the SRRs and the dielectric constant of the substrate.

The resonant frequency f_0 of the open resonator ring can be calculated by

$$f_0 = \frac{1}{2\pi}\sqrt{\frac{1}{L_T C_{eq}}} \tag{1}$$

where C_{eq} is the equivalent distributed capacitance of the entire open resonator ring. The distributed capacitance can be obtained by calculating the distributed capacitance between the two rings of the SRR and the capacitance across the gap. The calculation formula is given by

$$C_{eq} = \left(2a_{avg} - \frac{g}{2}\right) C_{pul} + \frac{\varepsilon_0 c t_m}{2g} \tag{2}$$

where c and t_m are the width and thickness of the metal ring; d is the gap distance between the two rings; and ε_0 is the vacuum permittivity. The size of the gap in the open resonator ring is denoted by g, and the average ring size a_{avg} can be obtained from Equation (3)

$$a_{avg} = a_{ext} - c - \frac{d}{2} \tag{3}$$

where a_{ext} is the length of the open resonator ring. C_{pul} is the capacitance per unit length, calculated by

$$C_{pul} = \frac{\sqrt{\varepsilon_e}}{c_0 Z_0} \tag{4}$$

where $c_0 = 3 \times 10^8$ m/s, ε_e is the effective dielectric constant of the medium, and Z_0 is the transmission line's characteristic impedance. Equation (5) is used to calculate the equivalent inductance L_T of a rectangular cross-section wire with finite length and thickness.

$$L_T = 0.0002l\left(2.303\log_{10}\frac{4l}{c} - r\right) uH \tag{5}$$

$r = 2.85$ is the geometric constant for a square SRR. The length of the metal wire l can be calculated by

$$l = 8a_{ext} - g \tag{6}$$

By Equations (1)–(6), the resonant frequency of the SRR can be calculated, which is determined by its geometric parameters c, g, and d, as well as the dielectric constant of the substrate.

At the resonant frequency of the open resonator ring, the propagated signal is suppressed and reflected. To achieve the multi-stopband effect of the antenna, multiple SRRs with different geometric dimensions and resonant frequencies can be alternately placed parallel to the CPW transmission line. In this design, the two pairs of open resonator rings are separated along the axis of the transmission line, with a distance of $\lambda/4$, where λ is the wavelength corresponding to the minimum resonant frequency. The monopole antenna radiator and the SRR are designed independently. Multiple SRRs can be used to adjust the desired stopbands as needed within the spectrum range of the UWB antenna radiation.

The prototype monopole antenna and UWB bandstop antenna structure shown in Figures 1 and 2 were simulated using the electromagnetic simulation software HFSS. The obtained reflection coefficient S_{11} results are shown in Figure 3. It can be observed that the prototype monopole antenna achieved a reflection coefficient of $S_{11} < -10$ dB within the range of 2.8 GHz to 12 GHz. The UWB bandstop antenna,

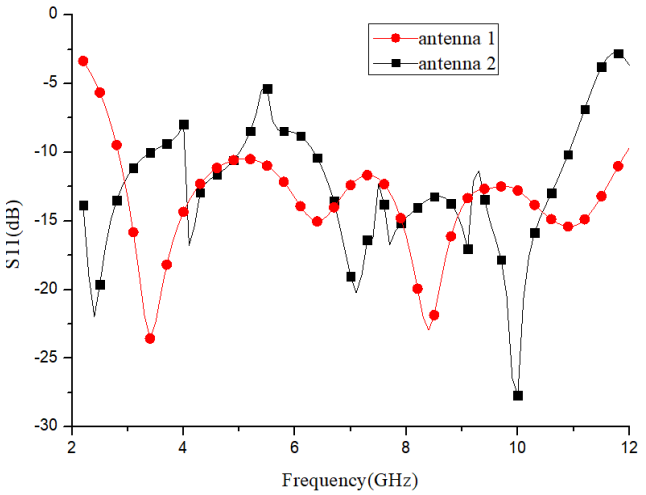

FIGURE 3. Simulation results of reflection coefficients of monopole antenna 1 and UWB bandstop antenna 2.

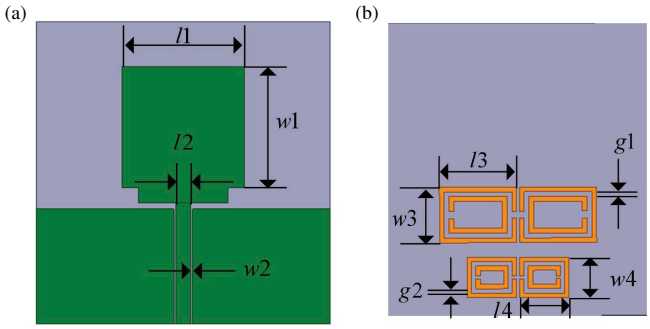

FIGURE 4. Dimension diagram of the antenna. (a) Front, (b) back.

TABLE 1. Dimensional parameters of the antenna.

Parameter	Unit (mm)	Parameter	Unit (mm)
$l1$	15	$w2$	0.25
$l2$	1.8	$w3$	7.6
$l3$	10.6	$w4$	5.5
$l4$	6.8	$g1$	0.65
$w1$	17.5	$g2$	0.6

on the other hand, achieved a reflection coefficient $S_{11} < -10$ dB within the ranges of 2.1 GHz to 3.3 GHz, 4.1 GHz to 5.1 GHz, and 6.3 GHz to 10.8 GHz. Furthermore, it exhibited good stopband characteristics within the frequency ranges of 3.3 GHz to 4 GHz and 5.1 GHz to 6.2 GHz, effectively suppressing interference from WiMAX (3.3 GHz–3.8 GHz) and WLAN (5.15 GHz–5.825 GHz) in the UWB wireless communication system. The dimensions of the designed antenna were 40 mm × 36 mm × 1 mm, and Table 1 provides specific parameters of the physical dimensions of the UWB bandstop antenna. The front and back views of the antenna are depicted in Figure 4, and the fabricated prototype of the antenna is shown in Figure 5.

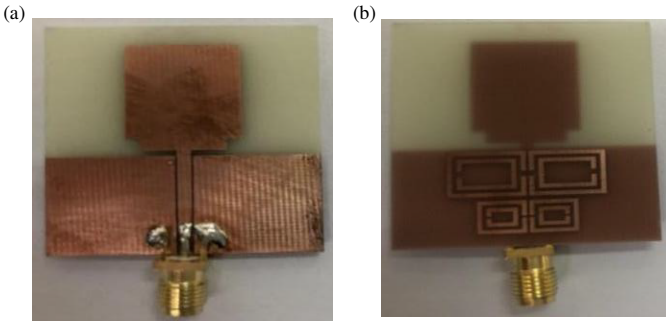

FIGURE 5. Physical fabrication diagram of the antenna. (a) Front, (b) back.

Figure 6 shows the measured reflection coefficient S_{11} of the antenna using the vector network analyzer Agilent E8363C. The measured bandwidth with a reflection coefficient less than −10 dB is 2.2 GHz to 3.3 GHz, 4.3 GHz to 5.1 GHz, and 6.3 GHz to 10.8 GHz. The measured stopband bandwidth is 3.3 GHz to 4.3 GHz and 5.1 GHz to 6.5 GHz. Comparing the simulation and measurement results, they are relatively consistent, but some discrepancies are still present. The reason for this deviation may be variations in the height of the fabricated substrate or issues with the precision of the fabrication process.

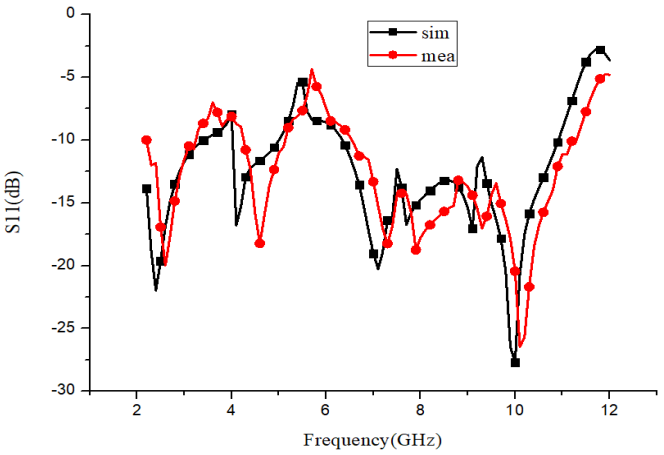

FIGURE 6. Simulation and measurement results of the S_{11} parameter for the antenna.

The ultra-wide bandstop antenna needs to exhibit bandstop characteristics and requires good radiation patterns throughout the entire frequency range. Figure 7 presents the normalized far-field radiation patterns of the designed antenna at 2.8 GHz, 7 GHz, and 9 GHz in the E-plane and H-plane. It can be observed that the antenna has low cross-polarization in the main radiation direction. The axial gains at these three frequencies are 2.8 dBi, 4.8 dBi, and 5.5 dBi, respectively.

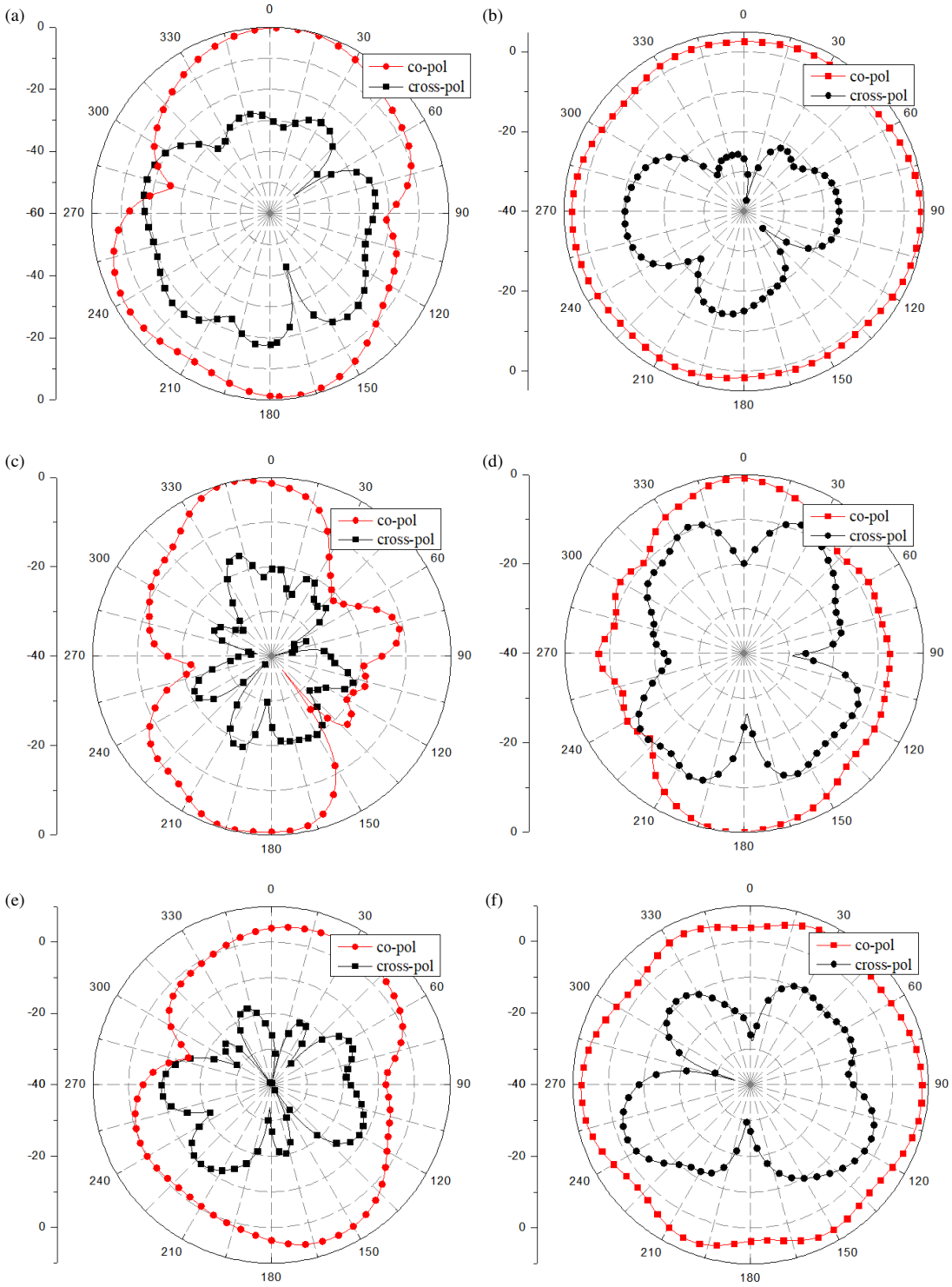

FIGURE 7. The far-field diagram of the antenna radiating E-plane and H-plane at 2.8 GHz, 7 GHz, and 9 GHz. (a) 2.8 GHz E-plane, (b) 2.8 GHz H-plane, (c) 7 GHz E-plane, (d) 7 GHz H-plane, (e) 9 GHz E-plane, (f) 9 GHz H-plane.

3. CONCLUSION

To effectively suppress frequency interference between ultra-wideband (UWB) systems and global microwave interconnect networks such as WiMAX and WLAN, a dual-bandstop UWB antenna was designed in this study. By loading two pairs of open resonator rings (SRRs) on the coplanar waveguide (CPW) ground plane, the antenna achieved bandstop effects within two frequency bands, namely (3.275 GHz to 4.05 GHz) and (4.95 GHz to 6.25 GHz). This design effectively suppressed the interference from WiMAX (3.3 GHz to 3.8 GHz) and WLAN (5.15 GHz to 5.825 GHz) in wireless communication systems. Through fabrication and measurement of the antenna's reflec-

tion coefficient, it was found that the simulation and measurement results were consistent. Moreover, the antenna exhibited favourable radiation characteristics, making it suitable for future wireless communication devices.

ACKNOWLEDGEMENT

This work is supported by the Chengdu Green and Low-Carbon Development Research Base Project (Grant No. LD2024Z47), Meteorological Disaster Prediction, Early Warning, and Emergency Management Research Center Project (Grant No. ZHYJ23-YB07), and Research Base Project for Refined Governance of Megacities (Grant No. TD2023Z06).

REFERENCES

[1] Ghiasvand, F., "UWB full polarization single-plane monopulse reflector antenna," *Electromagnetics*, Vol. 43, No. 1, 1–13, 2023.

[2] Li, H., H. Zhang, Y. Kong, and C. Zhou, "Flexible dual-polarized UWB antenna sensors for breast tumor detection," *IEEE Sensors Journal*, Vol. 22, No. 13, 13 648–13 658, 2022.

[3] Lakshmaiah, Y. V. and B. Roy, "Planar monopole antenna based on surface roughness and stub loaded with notch controlling characteristics," *Transactions on Electrical and Electronic Materials*, Vol. 24, No. 6, 502–510, 2023.

[4] Wang, Z., R. You, M. Yang, J. Zhou, and M. Wang, "Design of a monopole antenna for WiFi-UWB based on characteristic mode theory," *Progress In Electromagnetics Research M*, Vol. 125, 107–116, 2024.

[5] Nawati, V. R., B. K. Sujatha, G. S. Karthikeya, A. Desai, H. T. Hsu, and M. Palandoken, "A compact dual-polarized probe-fed UWB antenna system for breast cancer detection applications," *Wireless Networks*, Vol. 30, 3039–3050, 2024.

[6] Siddiqui, J. Y., C. Saha, and Y. M. M. Antar, "Compact dual-SRR-loaded UWB monopole antenna with dual frequency and wideband notch characteristics," *IEEE Antennas and Wireless Propagation Letters*, Vol. 14, 100–103, 2015.

[7] Ali, M. M. M., A. A. R. Saad, and E. E. M. Khaled, "A design of miniaturized ultra-wideband printed slot antenna with 3.5/5.5 GHz dual band-notched characteristics: Analysis and implementation," *Progress In Electromagnetics Research B*, Vol. 52, 37–56, 2013.

[8] Wang, J. H., Z. Wang, Y.-Z. Yin, and X. Liu, "UWB monopole antenna with triple band-notched characteristic based on a pair of novel resonators," *Progress In Electromagnetics Research C*, Vol. 49, 1–10, 2014.

[9] Peddakrishna, S. and T. Khan, "Design of UWB monopole antenna with dual notched band characteristics by using π-shaped slot and EBG resonator," *AEU — International Journal of Electronics and Communications*, Vol. 96, 107–112, 2018.

[10] Luo, C.-M., J.-S. Hong, and H. Xiong, "A tri-band-notched UWB antenna with low mutual coupling between the band-notched structures," *Radioengineering*, Vol. 22, No. 4, 1233–1238, 2013.

[11] Siddiqui, J. Y., C. Saha, and Y. M. M. Antar, "Compact SRR loaded UWB circular monopole antenna with frequency notch characteristics," *IEEE Transactions on Antennas and Propagation*, Vol. 62, No. 8, 4015–4020, 2014.